CHiP Annual Meeting on 2023

Research of Laser-Driven High-Order Harmonic Generation

Hsu-hsin Chu (朱旭新)
Associated Professor
2023/11/24

Department of Physics, National Central University, Taiwan R.O.C.

The Nobel Prize in Physics 2023

Pierre Agostini
The Ohio State University, USA

Ferenc Krausz
Max Planck Institute of Quantum Optics, Germany

Anne L'Huillier
Lund University, Sweden

"for experimental methods that generate attosecond pulses of light for the study of electron dynamics in matter"

attosecond science

Homemade 100-TW laser system at NCU

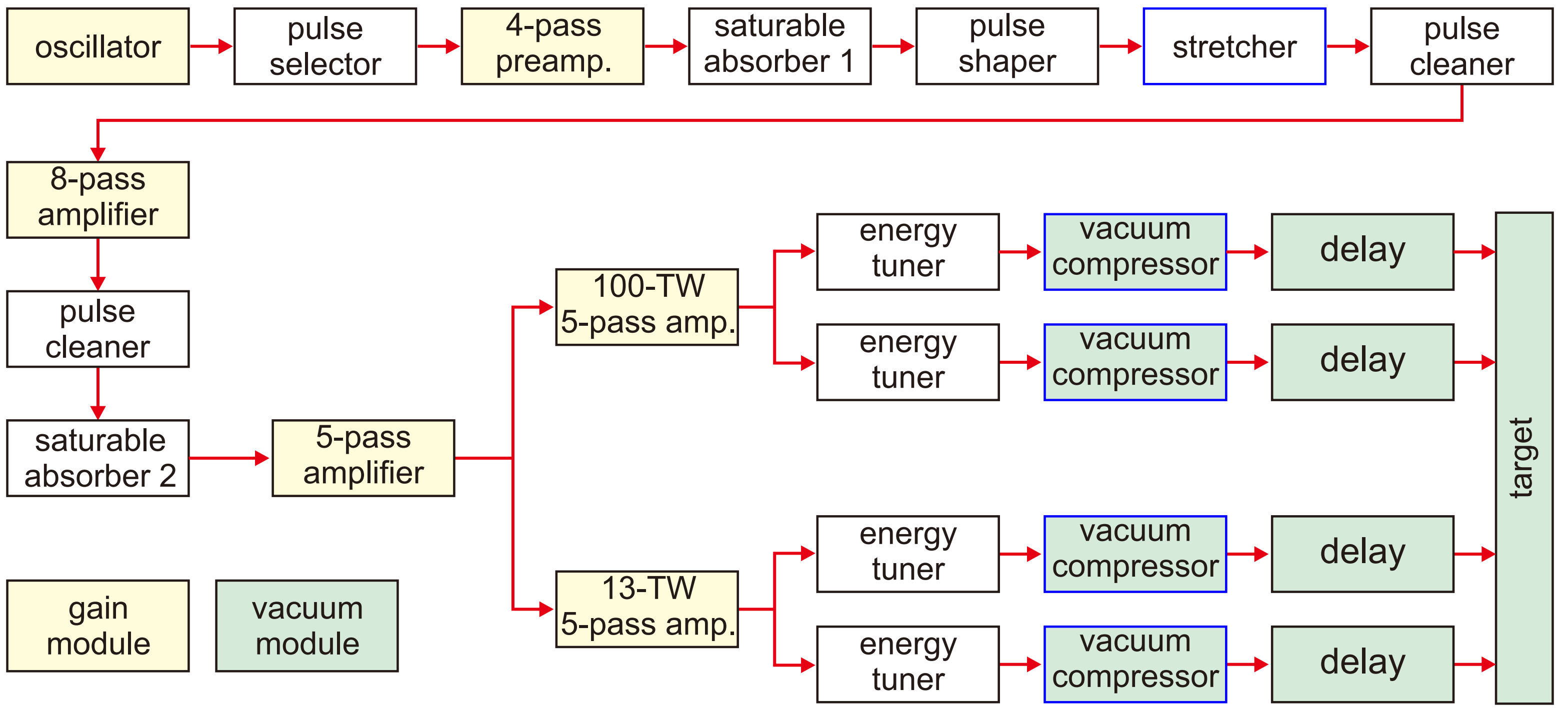

- wavelength = 810 nm
- pulse energy = 3 J
- pulse duration = 30 fs
- peak power = 100 TW
- focused intensity > 10^{20} W/cm^2

30 fs : 1 sec = 1 sec : 1M years

1 attosecond = 1/1000 fs

High-order harmonic generation (HHG)

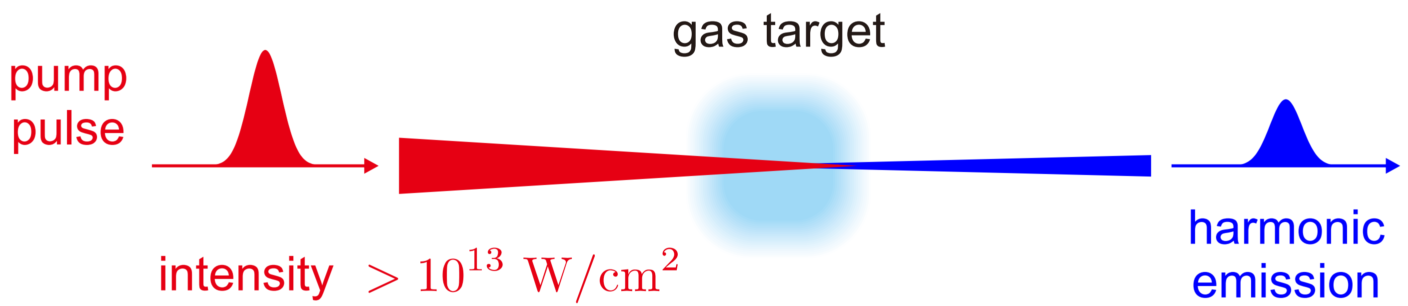

- HHG spectrum:

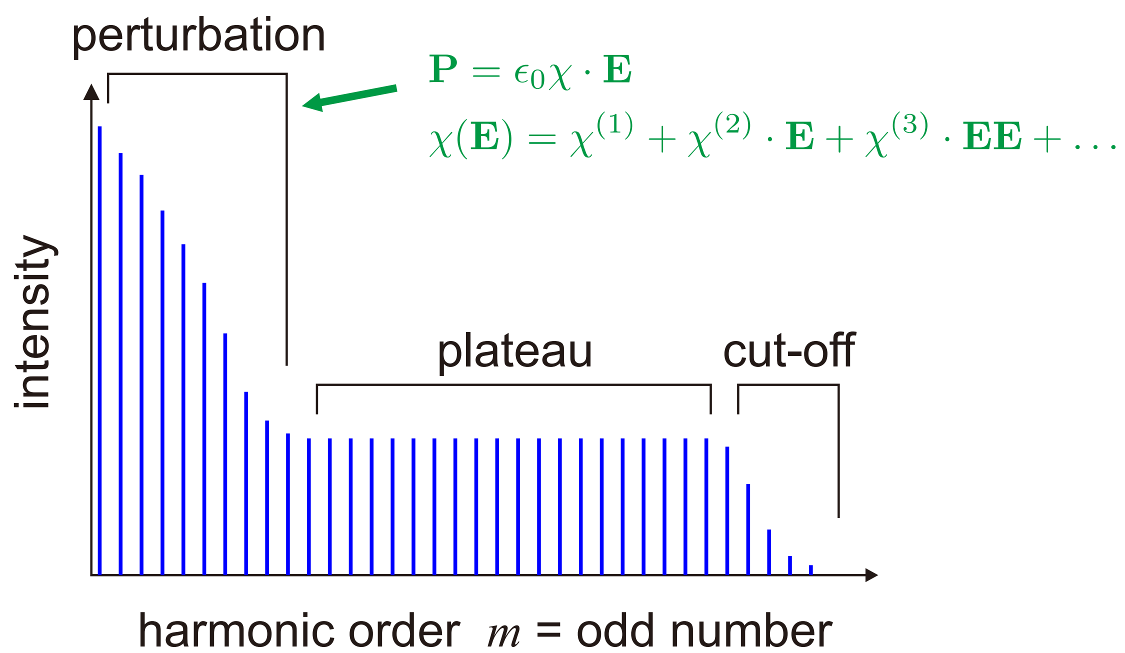

Three-step model of HHG

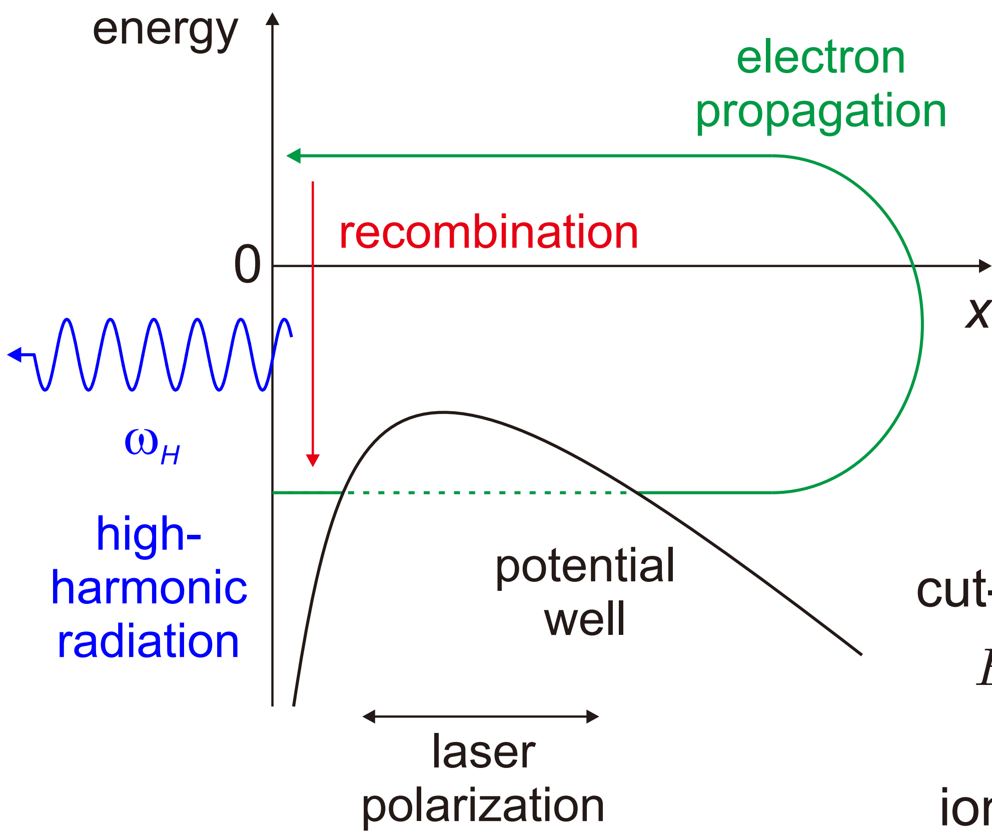

- tunnelling-ionization resulted by pump laser
- acceleration of the ionized electron
- recombination and HHG emission

cut-off energy:

$$E_{\max} = I_p + 3.17\,U_p$$

ionization potential ponderomotive potential

Electron trajectory

■ electron trajectory

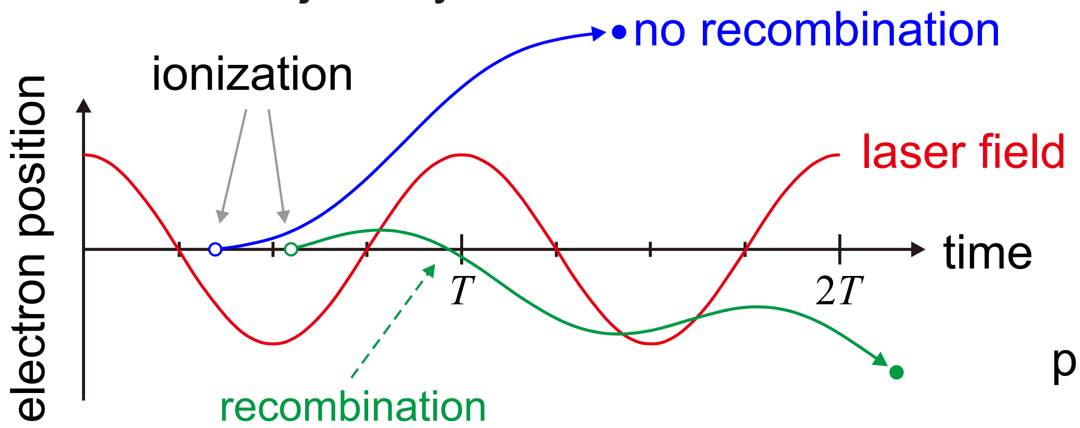

pulse train separation
= 1/2 laser period

spectrum separation
= 2x laser frequency

■ HHG emission

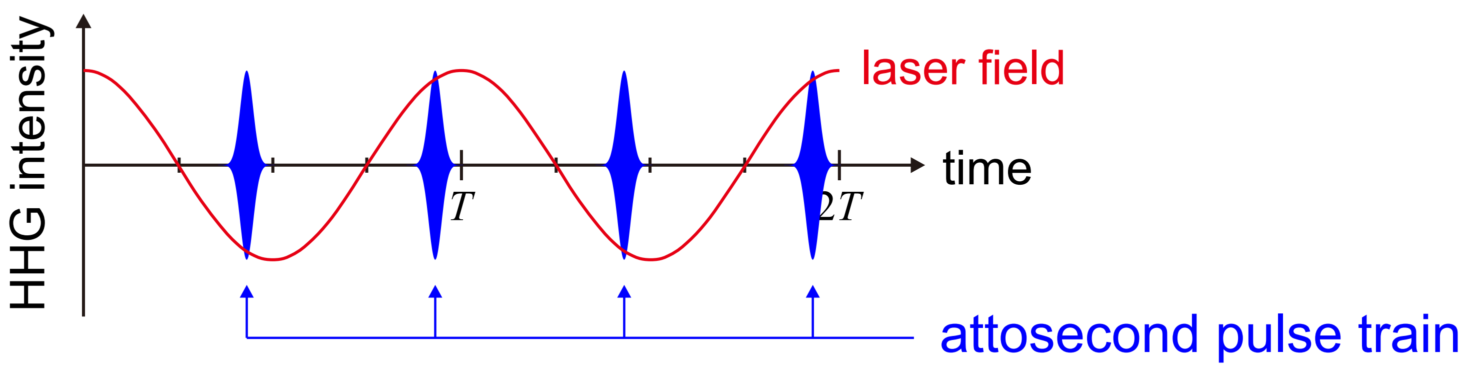

Output photon energy

- electron kinetic energy at recombination

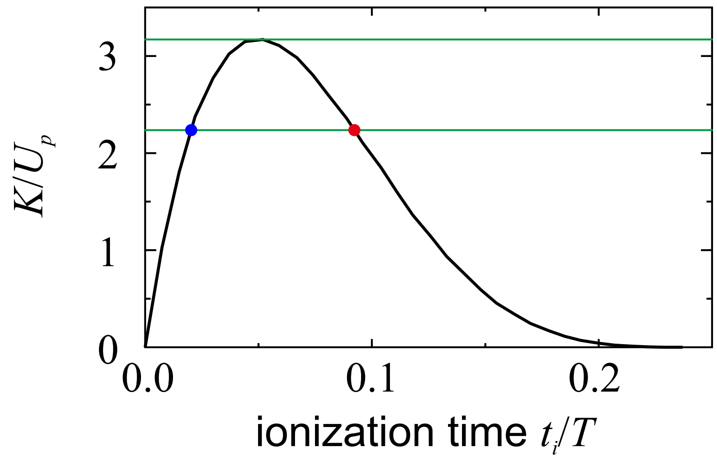

cutoff photon energy:

$$E_{\max} = I_p + 3.17\,U_p$$

For a specific harmonic order, there exists two possible electron trajectories.

- electron trajectory

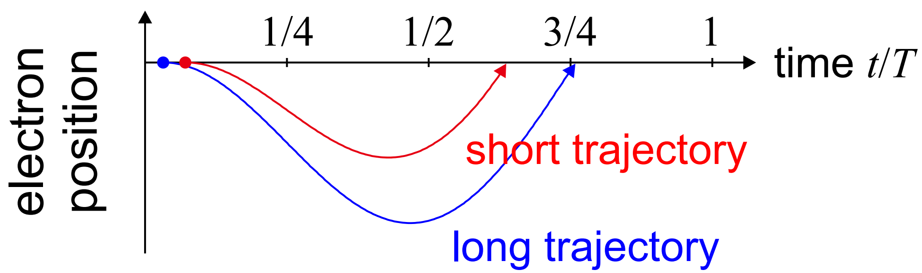

Generation of attosecond pulses

- pumping by a long pulse

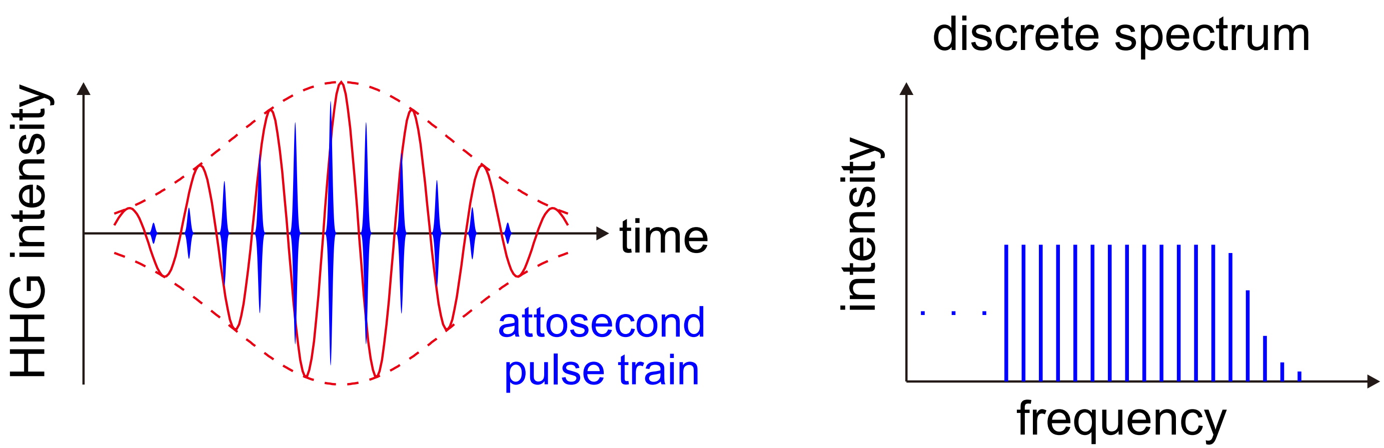

- pumping by a few-cycle pulse

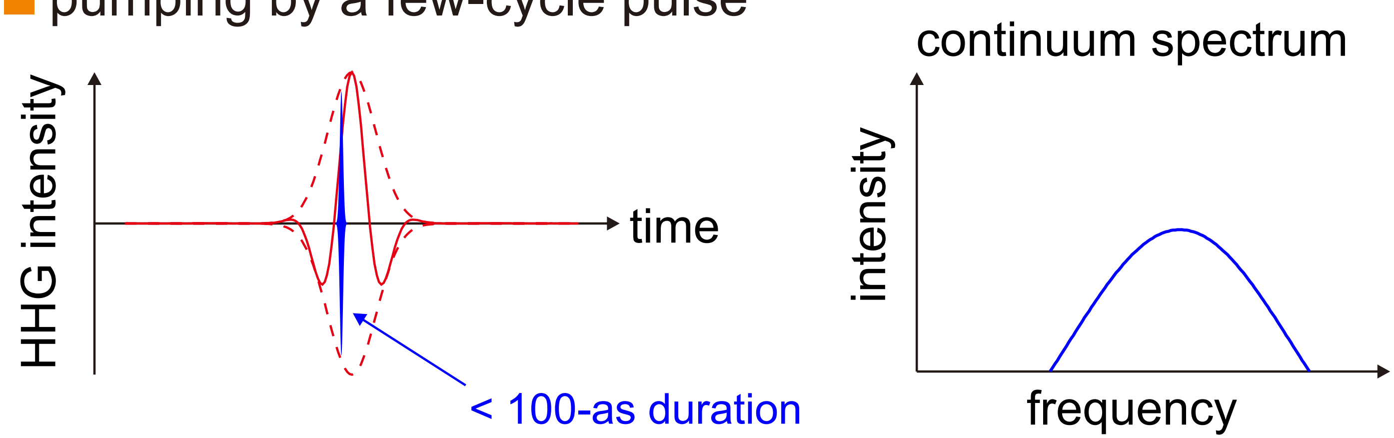

Time scales of different processes

events	time scale
human racing, mechanical shutter	millisecond
fast protein folding	microsecond
fast circuits, molecule rotation	nanosecond
slow molecule vibration	picosecond
chemical reaction, electron transition	femtosecond
inter-atom electron evolution	attosecond

- Ultrashort optical pulses can be applied to resolve the dynamics of very fast processes.

High-harmonic generation from Ar gas

raw data form x-ray imaging spectrometer

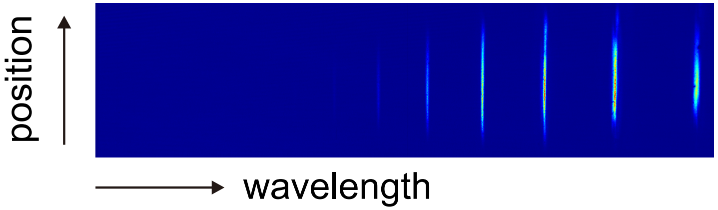

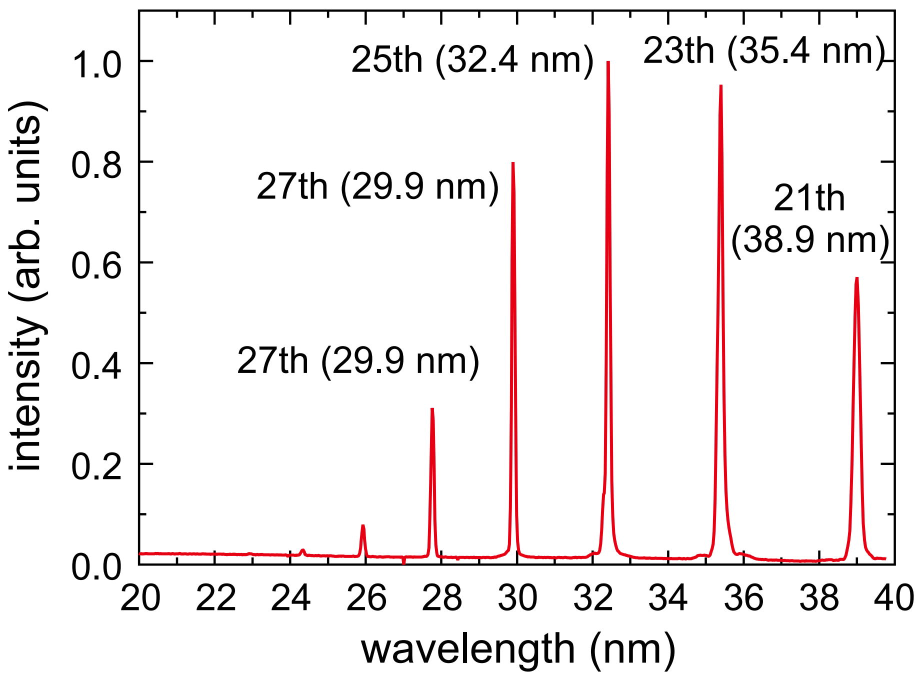

- condition:

  pump energy = 7 mJ

  pump wavelength = 810 nm

  pump duration = 45 fs

  peak intensity

  $= 5.6 \times 10^{14}$ W/cm^2

  nozzle diameter = 2 mm

  backing pressure = 70 psi

  atom density = 1×10^{18} cm^{-3}

- the 25th harmonics:

  wavelength = 32.4 nm

  photon number = 1.26×10^8

  pulse energy = 0.77 nJ

  conversion efficiency

  $= 1.1 \times 10^{-7}$

High-harmonic generation from Ar gas

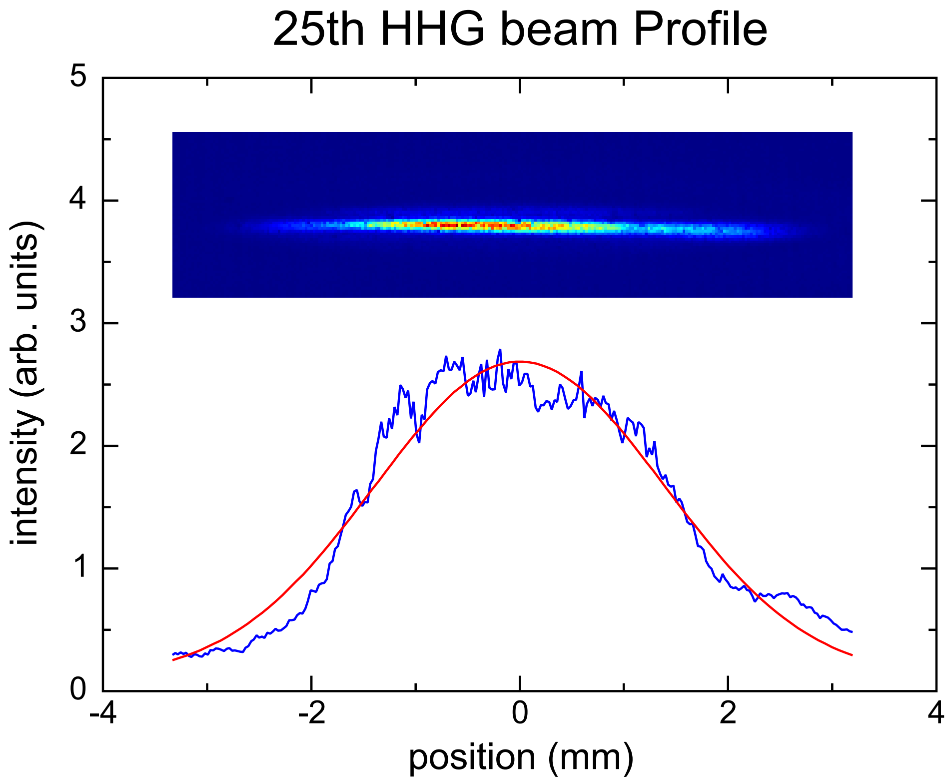

- the 25th harmonics:

wavelength
= 32.4 nm
beam diameter
= 3.28 mm (FWHM)
beam divergaence
= 1.33 mrad
pulse energy
= 0.77 nJ
source diameter
= 150 μm (FWHM)
pulse duration
= 45 fs

peak spectral brightness = 3.7×10^{22} photons/sec/mm^2/mrad^2/0.1%BW
(NSRRC U9 beamline = 5×10^{18} photons/sec/mm^2/mrad^2/0.1%BW)

peak photon flux = 9.1×10^{20} photons/sec/0.1%BW
(NSRRC U9 beamline = 1.5×10^{16} photons/sec/0.1%BW)

High-harmonic generation from He gas

imaging x-ray spectrometer

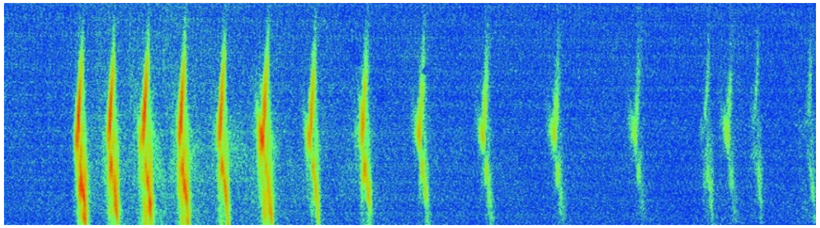

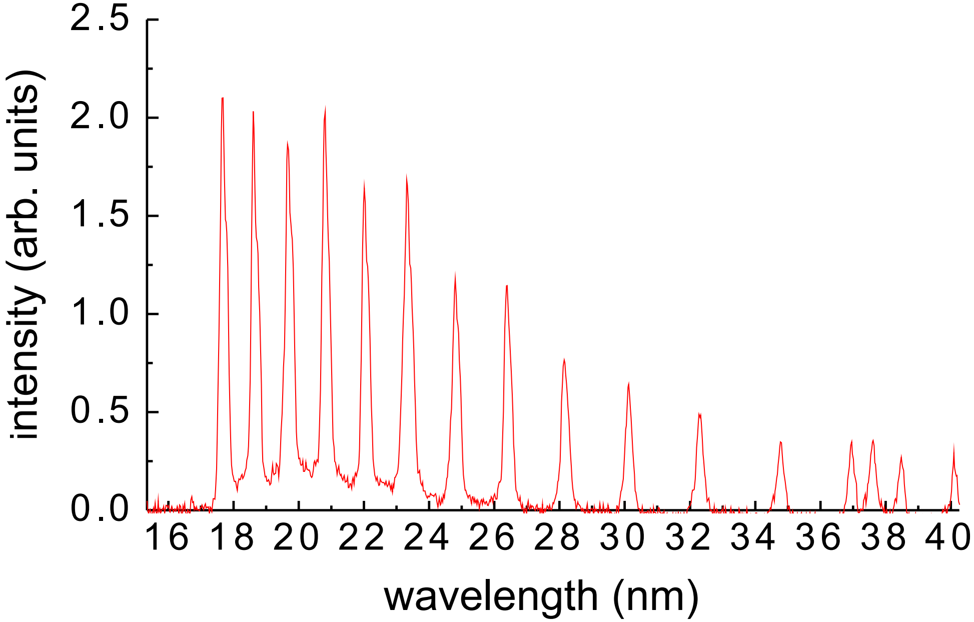

- condition:

  pump energy = 21 mJ

  pump wavelength = 810 nm

  pump duration = 37 fs

  peak intensity = 1.1×10^{16} W/cm^2

  atom density = 1.2×10^{20} cm^{-3}

- the 45th harmonic

  wavelength = 17.7 nm

  photon energy = 70 eV

  photon number = 3.1×10^6

  pulse energy = 0.035 nJ

  conversion efficiency = 1.7×10^{-9}

High-harmonic generation from He gas

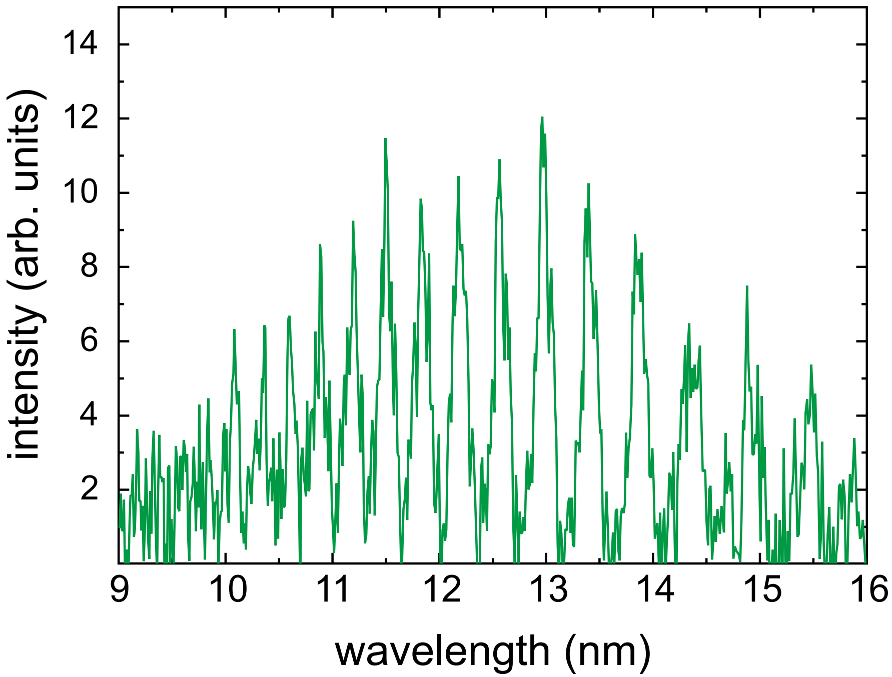

- condition:

  pump energy = 10.3 mJ

  pump wavelength = 810 nm

  pump duration = 35 fs

  peak intensity = 8.3×10^{15} W/cm^2

  atom density = 1.0×10^{19} cm^{-3}

- the 81st harmonic

  wavelength = 10.1 nm

  photon energy = 122.7 eV

  photon number = 2.3×10^3

  pulse energy = 0.045 pJ

  conversion efficiency = 4.3×10^{-12}

Phase-matching condition

■ phase matched

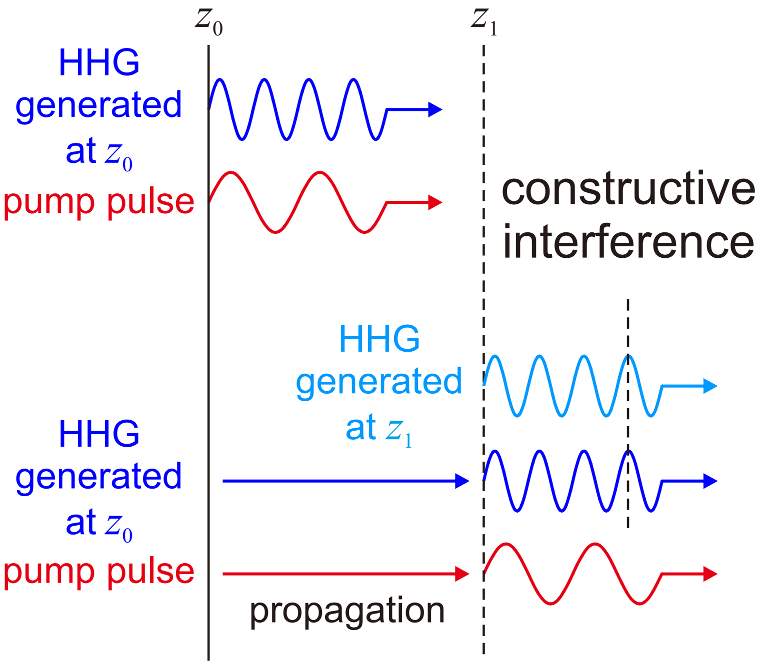

■ phase mismatched

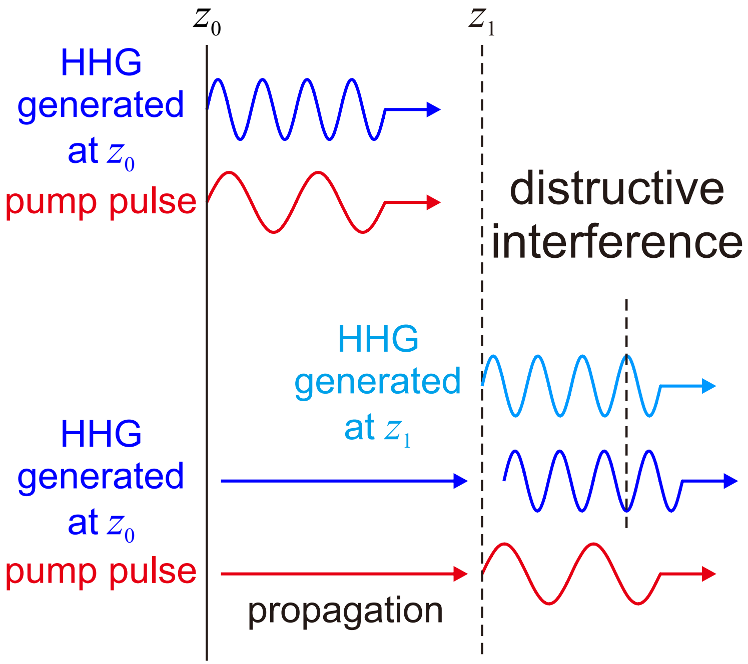

Phase-matching condition

- Generally the phase mismatch is represented by the wave-number mismatch.

$$\Delta k = qk(\omega_d) - k(\omega_q)$$

q: harmonic order

$\omega_q = q\omega_d$: harmonic frequency

ω_d: driving frequency

- The mismatch is resulted from the dispersion of gas and plasma, and the Gouy phase shift.

$$\Delta k = \Delta k_{\mathrm{gas}} + \Delta k_{\mathrm{plasma}} + \Delta k_{\mathrm{geo}} + \Delta k_{\mathrm{dipole}}$$

$$\begin{array}{cccc} \downarrow & \downarrow & \downarrow & \downarrow \\ (+) & (-) & (-) & (+/-) \end{array}$$

HHG intrinsic dipole phase

- It is an additional phase shift that arises from the process of ionization and recombination.

$$\Phi_{\text{dipole}}(q, I) = q\omega_0 t_r - \frac{1}{\hbar}\int_{t_i}^{t_r} \left(\frac{1}{2}m_e v(t')^2 + I_p\right) dt'$$

$$\begin{aligned} \Delta k_{\text{dipole}}(q, I) &= \frac{d\Phi_{\text{dipole}}}{dz} \\ &= \frac{d\Phi_{\text{dipole}}}{dI}\frac{dI}{dz} \end{aligned}$$

$$\frac{dI}{dz} > 0 \quad \Rightarrow \quad \Delta k_{\text{dipole}} < 0$$

$$\frac{dI}{dz} < 0 \quad \Rightarrow \quad \Delta k_{\text{dipole}} > 0$$

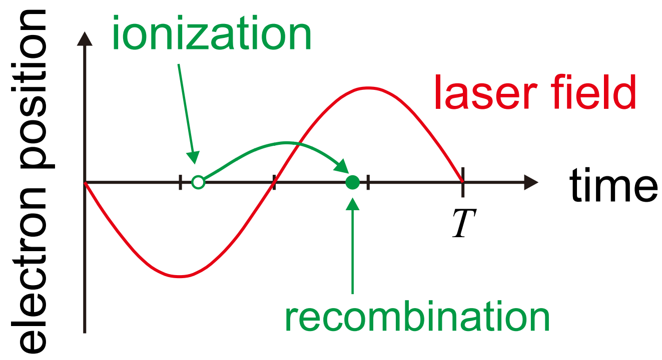

Optimization of EUV harmonic generation

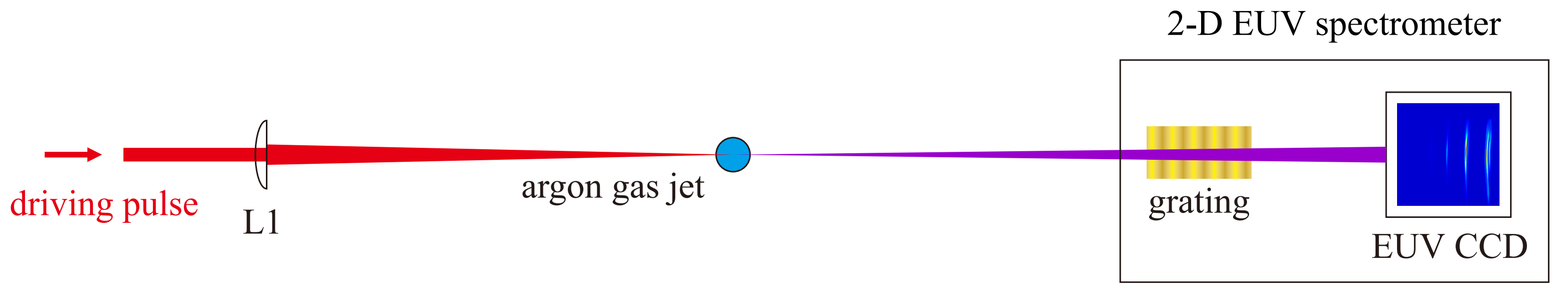

EUV spectrometer raw image

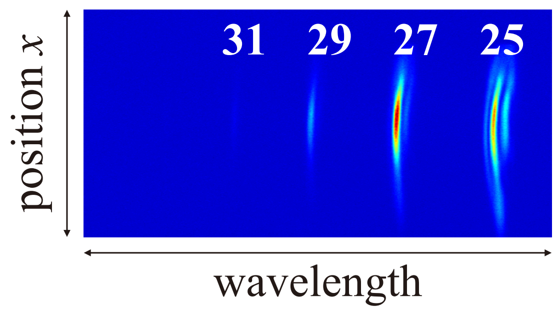

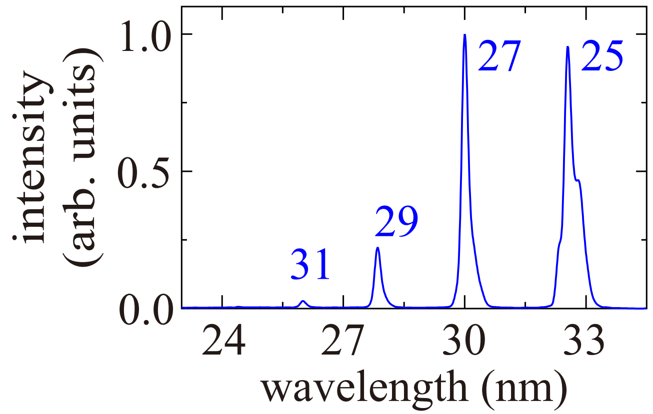

Tomography of the HHG process

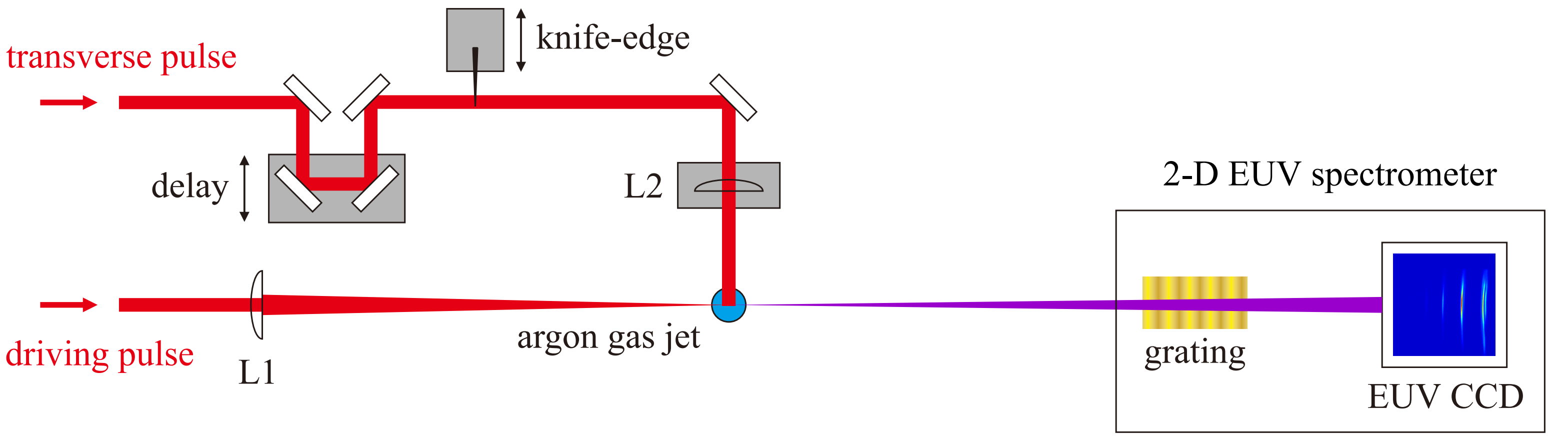

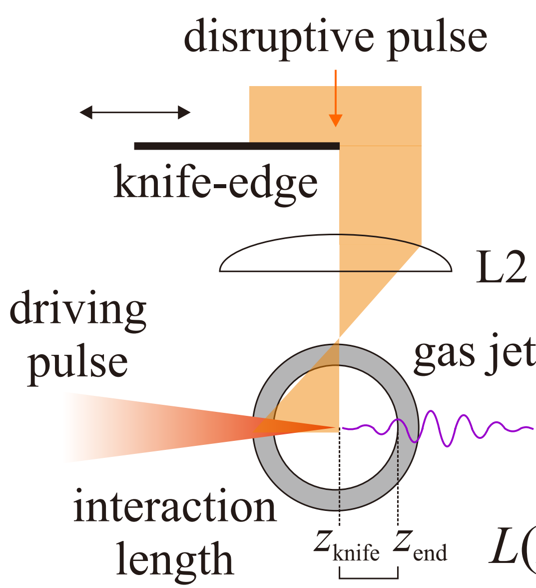

$$L(z_{\text{knife}}) = z_{\text{end}} - z_{\text{knife}}$$

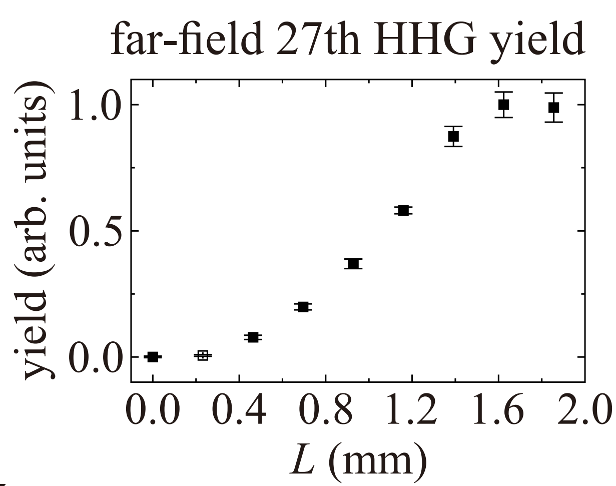

Suppression of harmonic generation

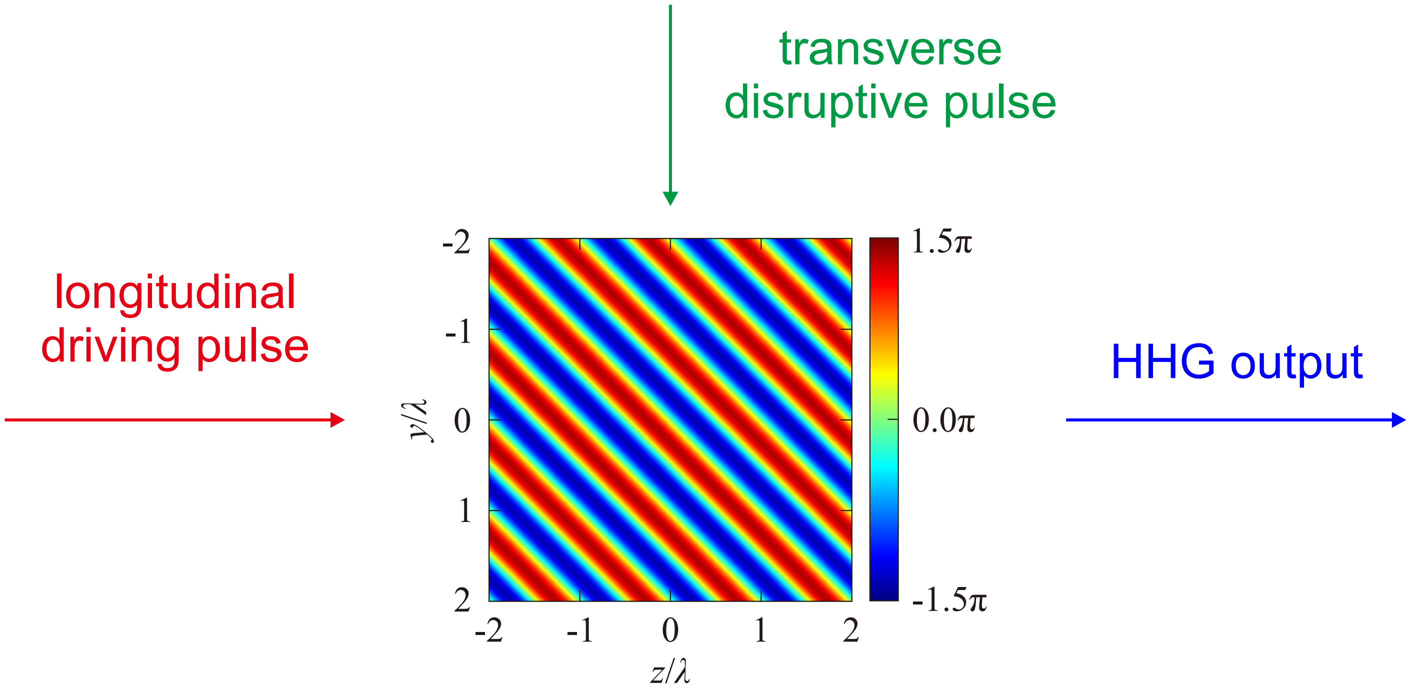

rapid phase modulation of the local harmonic field → suppression of the accumulated HHG

3-D phase-matching profile measurement

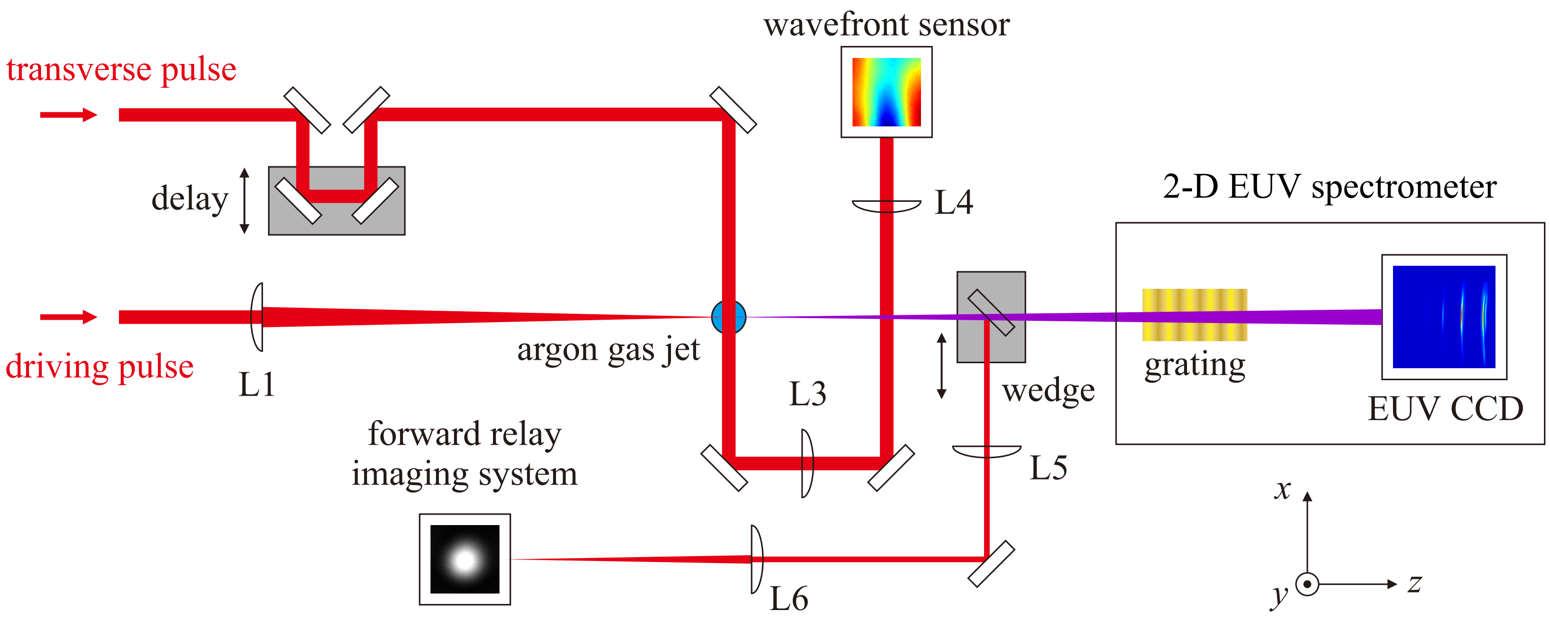

transverse wavefront seosor	➡	gas/plasma density distribution	➡	gas/plasma dispersion
loggitudinal relay-imaging system	➡	driving beam profile evolution	➡	Gouy phase/ dipole phase

3-D phase-matching profile measurement

neutral gas dispersion

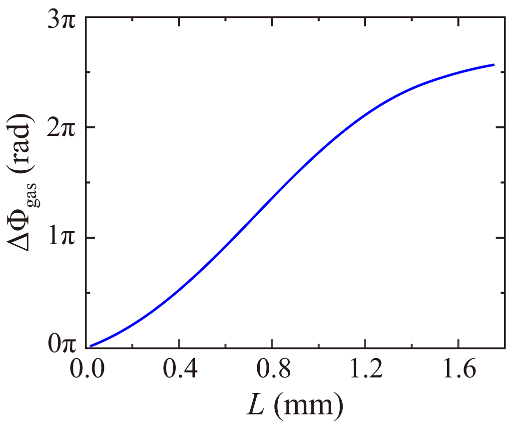

plasma dispersion

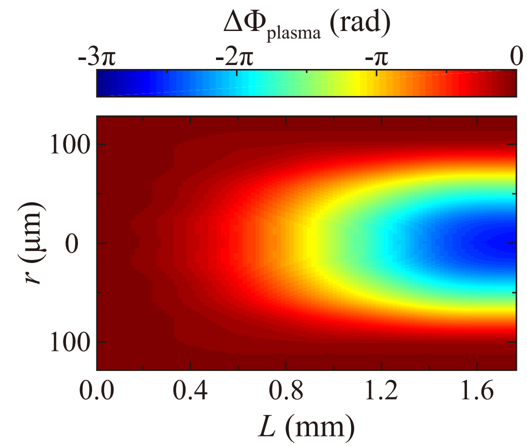

geomatrial phase shift

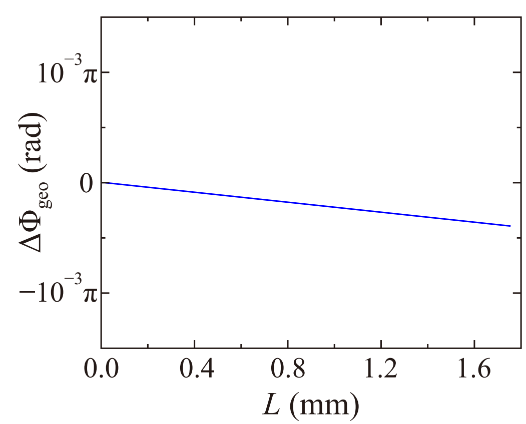

intrinsic dipole phase variation

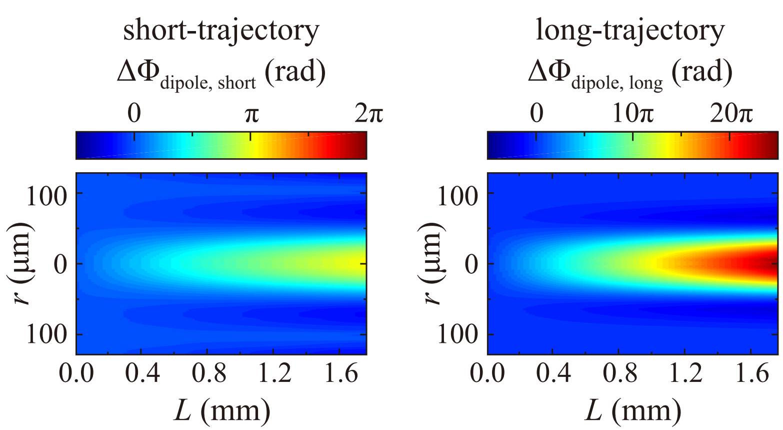

total accumulated phase mismatch

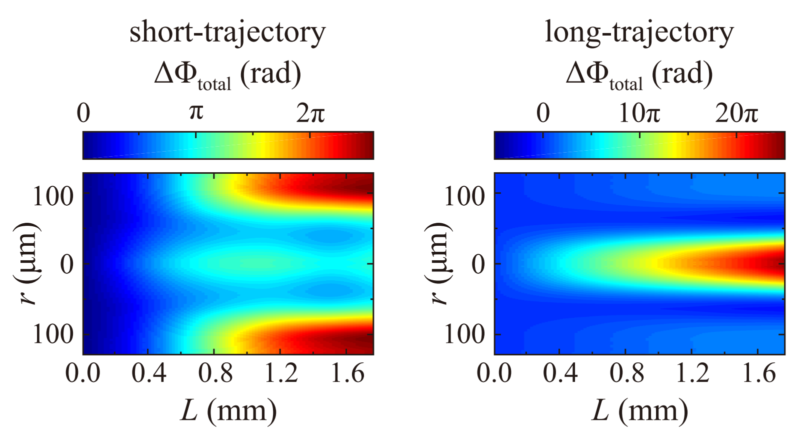

Reconstruction of the HHG growing curve

- Harmonic yield

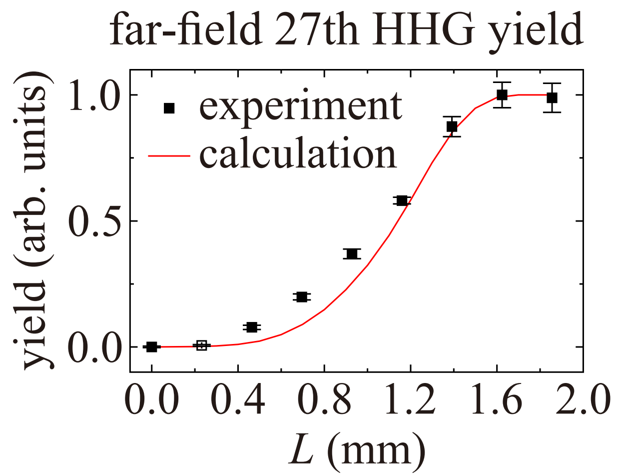

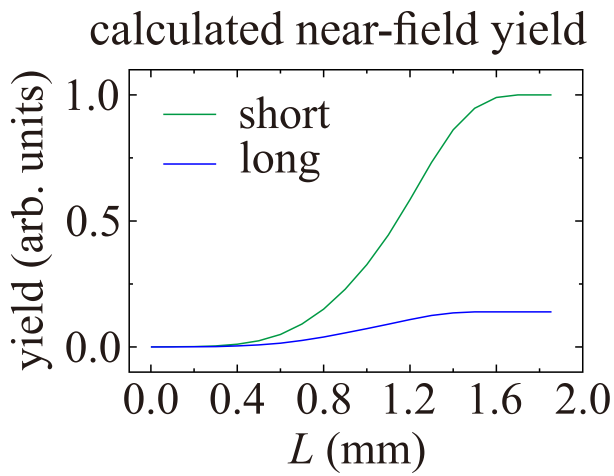

- The harmonic generation process is experimentally resolved in situ with complete 3-D phase matching profile measurement and tomography of the growing curve.

Ref: Phys. Rev. A **104**, 023112 (2021)

Toward keV hard x-ray harmonic generation

- Use ions as the interacting medium.

higher ionization potential → higher ionization intensity and thus higher U_p → higher cut-off photon energy

$$E_{\max} = I_p + 3.17\,U_p$$

He^{1+}: $I_p = 54.42$ eV	$I_d \sim 1.1 \times 10^{16}$ W/cm^2	~ 2 keV
Ne^{1+}: $I_p = 40.96$ eV	$I_d \sim 5.0 \times 10^{15}$ W/cm^2	~ 1 keV

- The plasma dispersion dominates the phase-matching condition.

- Control the dipole phase variation to achieve phase matching.

$$\Delta k = \underset{\text{(neglected)}}{\Delta k_{\text{gas}}} + \underbrace{\underset{(-)}{\Delta k_{\text{plasma}}} + \underset{(-)}{\Delta k_{\text{geo}}} + \underset{(+)}{\Delta k_{\text{dipole}}}}$$

$$\frac{dI}{dz} < 0$$

Using divergent driving pulse

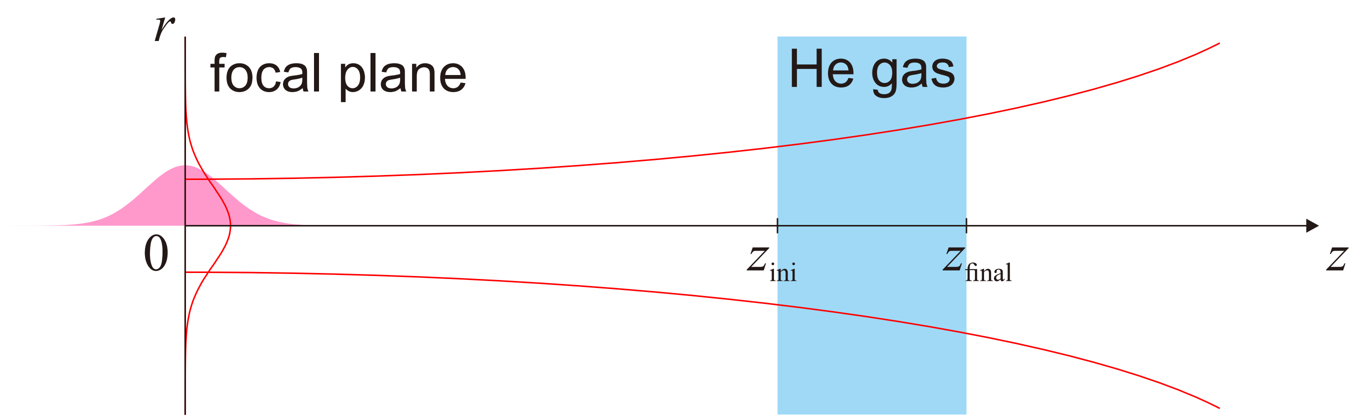

3-D Gaussian pulse

$$E(z,r,t) =$$

$$\frac{E_0}{2}\left[\left(\frac{-ib}{z-ib}\right)\exp\left(\frac{ikr^2}{2(z-ib)}\right)\exp\left(\frac{-(t-z/c)^2}{2\tau^2}\right)e^{i(kz-\omega t)}+\text{c.c.}\right]$$

$$E_0 = \sqrt{\frac{4\mu_0 c U_{\text{pulse}}}{\pi^{3/2}\tau w_0^2}}$$ peak electric field at the focal spot

U_{pulse} : pulse energy

w_0 : beam waist radius

τ : pulse duration

Propagation of the driving pulse

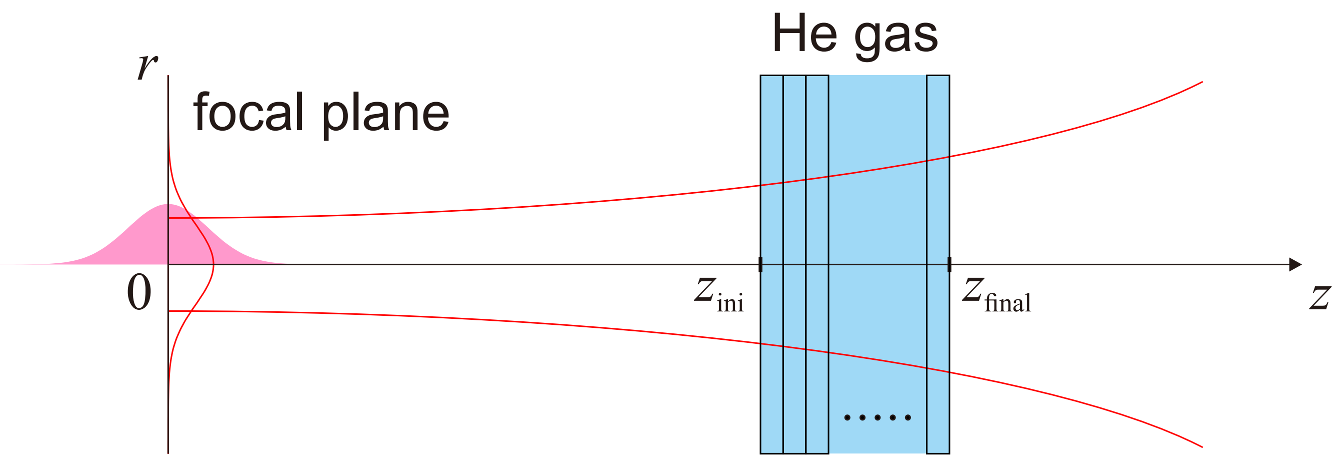

- Cut the gas distribution into a series of thin slices.
- Calculate the propagation of the driving pulse passing through each slice one by one, incorporating the effect of ionization, diffraction, and dispersion.

Propagation of the driving pulse

- transverse effects: natural diffraction and ionization defocusing

$E(z_j, r, t)$ is known.

Calculate the ionization at $r = 0$, $w(z_j)/2$, $w(z_j)$.

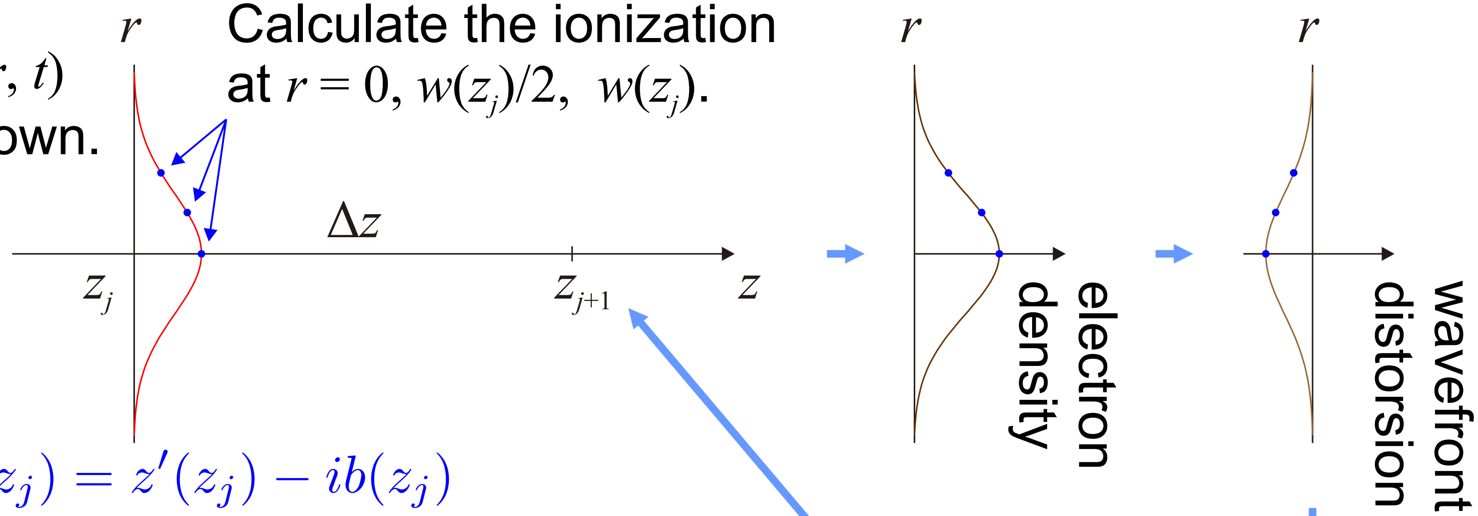

$$q(z_j) = z'(z_j) - ib(z_j)$$

$$\Phi_G(z_j) = -\tan^{-1}\left(\frac{z'(z_j)}{b(z_j)}\right)$$

$$R(z_j) = \frac{z'(z_j)^2 + b(z_j)^2}{z'(z_j)}$$

$$w(z_j) = \sqrt{\frac{2}{k}\left(\frac{z'(z_j)^2 + b(z_j)^2}{b(z_j)}\right)}$$

effective focal length f_j

Calculate $q(z_{j+1})$ from $q(z_j)$, f_j, and Δz.

Propagation of the driving pulse

- plasma dispersion

refractive index:

$$n_{\text{plasma}}(\omega, z_j) = \sqrt{1 - \frac{\omega_p(z_j)^2}{\omega^2}}$$

plasma frequency:

$$\omega_p(z_j) = \sqrt{\frac{q_e^2 N_e(z_j, r=0, t=\infty)}{\epsilon_0 m_e}}$$

wavenumber: $k_{\text{plasma}}(\omega, z_j) = \frac{\omega}{c} n_{\text{plasma}}(\omega, z_j)$

group delay from z_j to z_{j+1}:

$$\Delta C_{\text{plasma}}(\omega, z_j) = \frac{\partial k_{\text{plasma}}(\omega, z_j)}{\partial \omega} \Delta z = \frac{\Delta z}{c\, n_{\text{plasma}}(\omega, z_j)}$$

group-delay dispersion from z_j to z_{j+1}:

$$\Delta D_{\text{plasma}}(\omega, z_j) = \frac{\partial^2 k_{\text{plasma}}(\omega, z_j)}{\partial \omega^2} \Delta z = \frac{-\omega_p(z_j)^2 \Delta z}{c\left(\omega^2 - \omega_p(z_j)^2\right)^{3/2}}$$

Propagation of the driving pulse

- Dispersion due to Gouy phase shift

$$\phi_{\mathrm{Gouy}}(\omega, z) = -\tan^{-1}\left(\frac{z}{b}\right) = -\tan^{-1}\left(\frac{2cz}{w_0^2\omega}\right)$$

additional wavenumber due to Gouy phase shift:

$$k_{\mathrm{Gouy}} = \frac{\partial \phi_{\mathrm{Gouy}}(\omega, z)}{\partial z} = \frac{-2cw_0^2\omega}{4c^2z^2 + w_0^4\omega^2}$$

group delay from z = 0 to z:

$$C_{\mathrm{Gouy}} = \frac{\partial \phi_{\mathrm{Gouy}}(\omega, z)}{\partial \omega} = \frac{2cw_0^2 z}{4c^2z^2 + w_0^4\omega^2}$$

group-delay dispersion from z = 0 to z:

$$D_{\mathrm{Gouy}} = \frac{\partial^2 \phi_{\mathrm{Gouy}}(\omega, z)}{\partial \omega^2} = \frac{-4czw_0^6\omega}{\left(4c^2z^2 + w_0^4\omega^2\right)^2}$$

group-velocity dispersion:

$$\mathrm{GVD}_{\mathrm{Gouy}} = \frac{\partial D_{\mathrm{Gouy}}}{\partial z} = \frac{\partial^2 k_{\mathrm{Gouy}}}{\partial \omega^2} = \frac{4\omega\left(12c^3w_0^6z^2 - cw_0^{10}\omega^2\right)}{\left(4c^2z^2 + w_0^4\omega^2\right)^3}$$

Ionization loss

- Overcome the ionization potentials of the bound electrons.

$$\Delta U_{\mathrm{ionization}}(z) = [\, N_{\mathrm{gas}} I_{p1} + N_{\mathrm{He}^{2+}}(z) I_{p2}]\, \pi R^2 dz$$

I_{p1}: ionization potential of the helium first electron

I_{p2}: ionization potential of the helium second electron

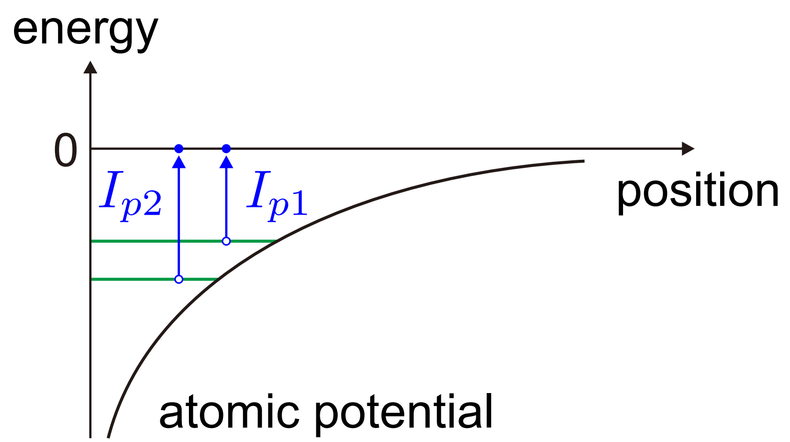

Above-threshold-ionization (ATI) heating

Electron is accelerated by the driving laser field directly.

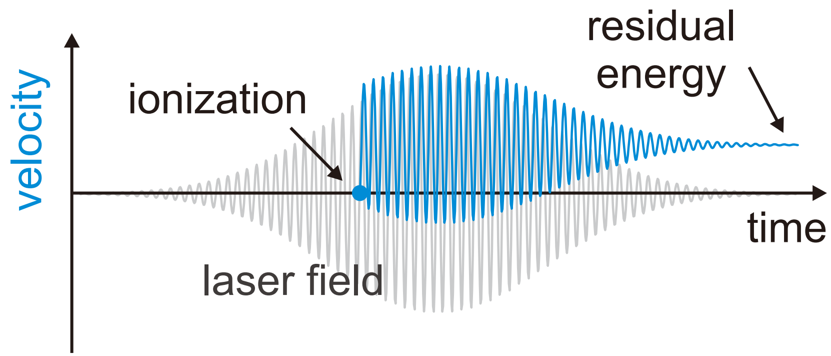

residual (absorbed) kinetic energy:

$$K_{\mathrm{ATI}}(z) = \frac{q_e^2 I_d(z,t_0)}{c\epsilon_0 m_e \omega_d^2} \sin^2(\omega_d t_0)$$

$I_d(z,t_0)$: driving laser intensity at the ionization time t_0

Inverse bremsstrahlung heating

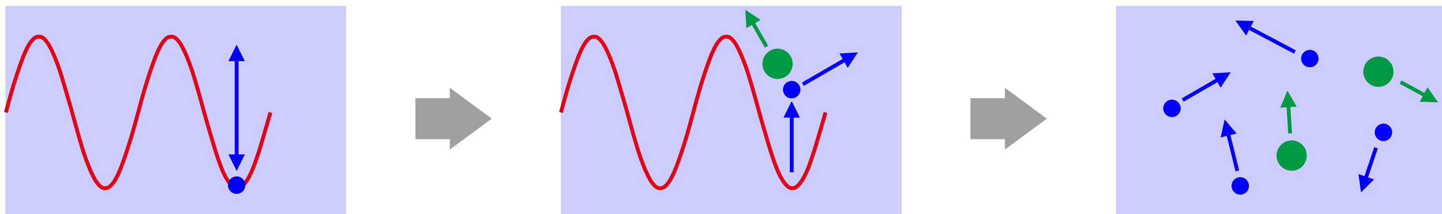

electron oscillation → electron-ion scattering → plasma thermal motion

attenuation coefficient:

$$a_{\mathrm{IB}}(z) = \frac{1}{3c\omega_d^2 n_{\mathrm{plasma}}(\omega_d, z)} \frac{q_e^6 Z(z) N_e(z)^2 \ln(\Lambda(z))}{2\pi\epsilon_0^2 m_e k_B T_e(z)^{3/2}}$$

$N_e(z)$: electron density

$T_e(z)$: electron temperature

Thomson scattering

Thomson scattering: scattering by free electron

attenuation coefficient:

$$a_{\mathrm{TS}}(z) = \frac{8\pi}{3} \frac{q_e^4}{(4\pi\epsilon_0 m_e c^2)^2} N_e(z)$$

Propagation of the driving pulse

- Driving laser field at z_{j+1}:

$$E(z_{j+1}, r, t) = E_{\mathrm{peak}}(z_{j+1}) \exp\left(\frac{ikr^2}{2q(z_{j+1})}\right) \exp\left(i \sum_{k=1}^{j} \left(k_{\mathrm{plasma}}(z_k)\Delta z + \Delta\phi_{\mathrm{Gouy}}(z_k)\right)\right) \times \exp\left(\frac{-(t - C(z_j))^2}{2\tau(z_{j+1})^2}\right) \exp\left(i\left(\frac{1}{2}\tan^{-1}\left(\frac{D(z_j)}{\tau_0^2}\right) - \frac{D(z_j)}{2\left(\tau_0^4 + D(z_j)^2\right)}(t - C(z_j))^2 - \omega t\right)\right)$$

peak electric field at z_{j+1}:

$$E_{\mathrm{peak}}(z_{j+1}) = \sqrt{\frac{4\mu_0 c U_{\mathrm{pulse}}(z_{j+1})}{\pi^{3/2}\tau(z_{j+1}) w(z_{j+1})^2}}$$

pulse duration at z_{j+1}:

$$\tau(z_{j+1}) = \sqrt{\tau_0^2 + \frac{D(z_j)^2}{\tau_0^2}}$$

accumulated group delay from z_{ini} to z_{j+1}: $C(j) = \sum_{k=1}^{j} \left(\Delta C_{\mathrm{plasma}}(k) + \Delta C_{\mathrm{Gouy}}(k)\right)$

accumulated GDD from z_{ini} to z_{j+1}: $D(j) = \sum_{k=1}^{j} \left(\Delta D_{\mathrm{plasma}}(k) + \Delta D_{\mathrm{Gouy}}(k)\right)$

Case 1: 655th (1 keV) harmonic generation

gas jet position z = 7~9.5 mm

pulse duration = 30 fs

wavelength = 810 nm

focal spot waist radius = 40 μm (b=6.2mm)

pulse energy = 35 mJ

He gas density = 1.33×10^{17} cm^{-3}

$z = z_{ini} = 7$ mm, r = 0.

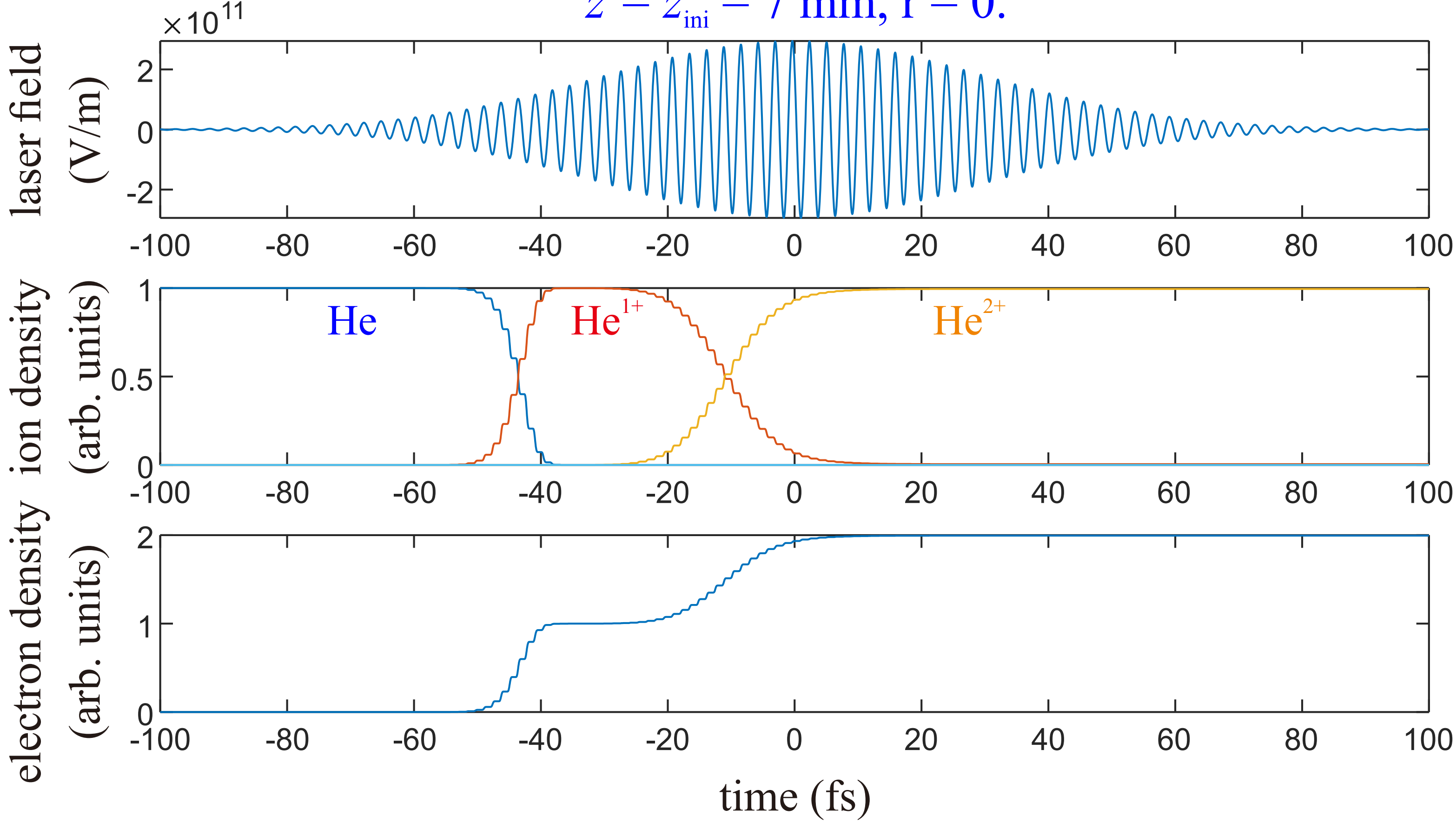

Case 1: 655th (1 keV) harmonic generation

gas jet position z = 7~9.5 mm: pulse duration = 30 fs wavelength = 810 nm

focal spot waist radius = 40 μm (b=6.2mm) pulse energy = 35 mJ He gas density = 1.33×10^{17} cm^{-3}

$z = z_{\mathrm{final}} = 9.5$ mm, r = 0.

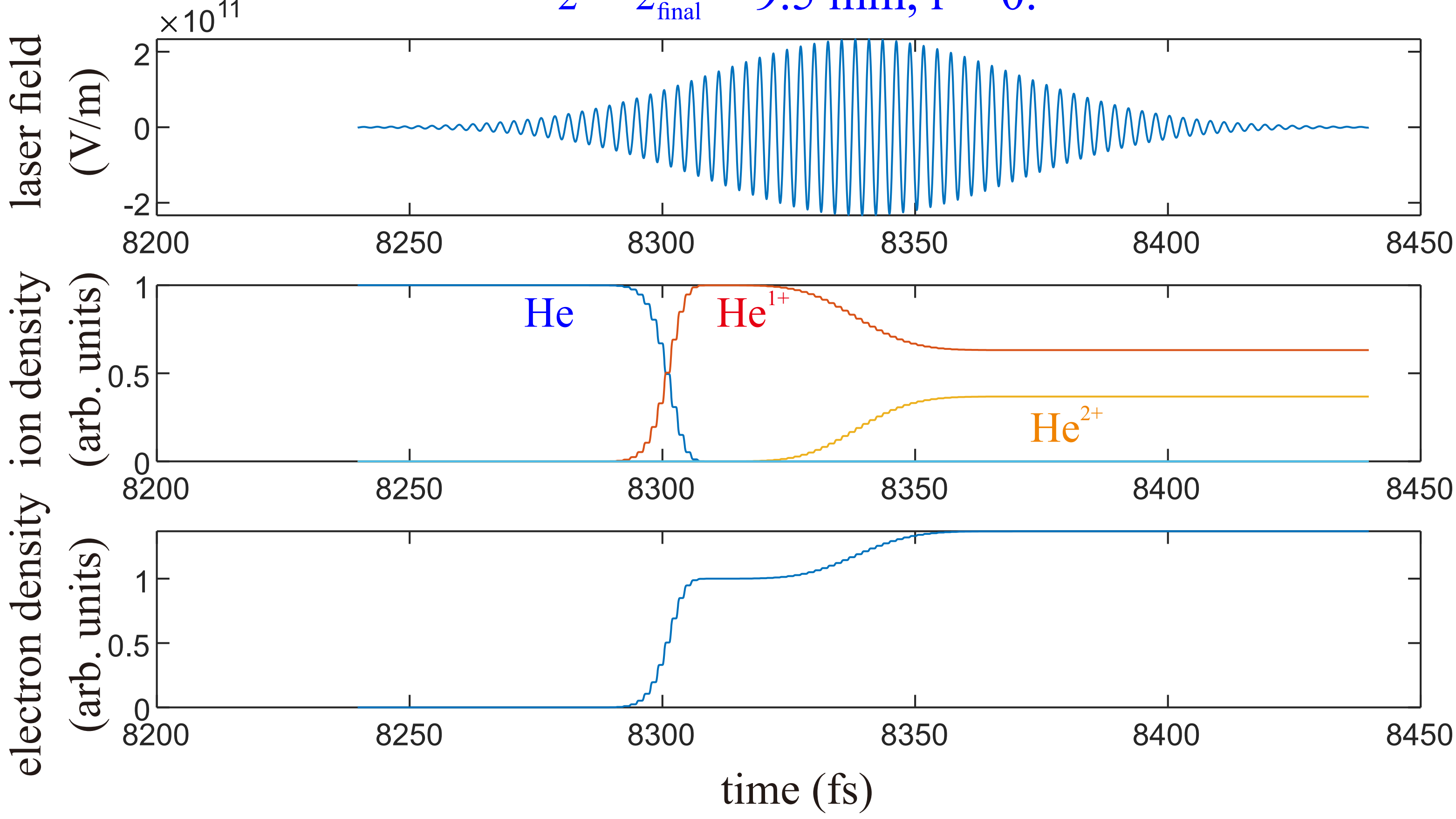

Case 1: 655th (1 keV) harmonic generation

final electron density after driving pulse passing through

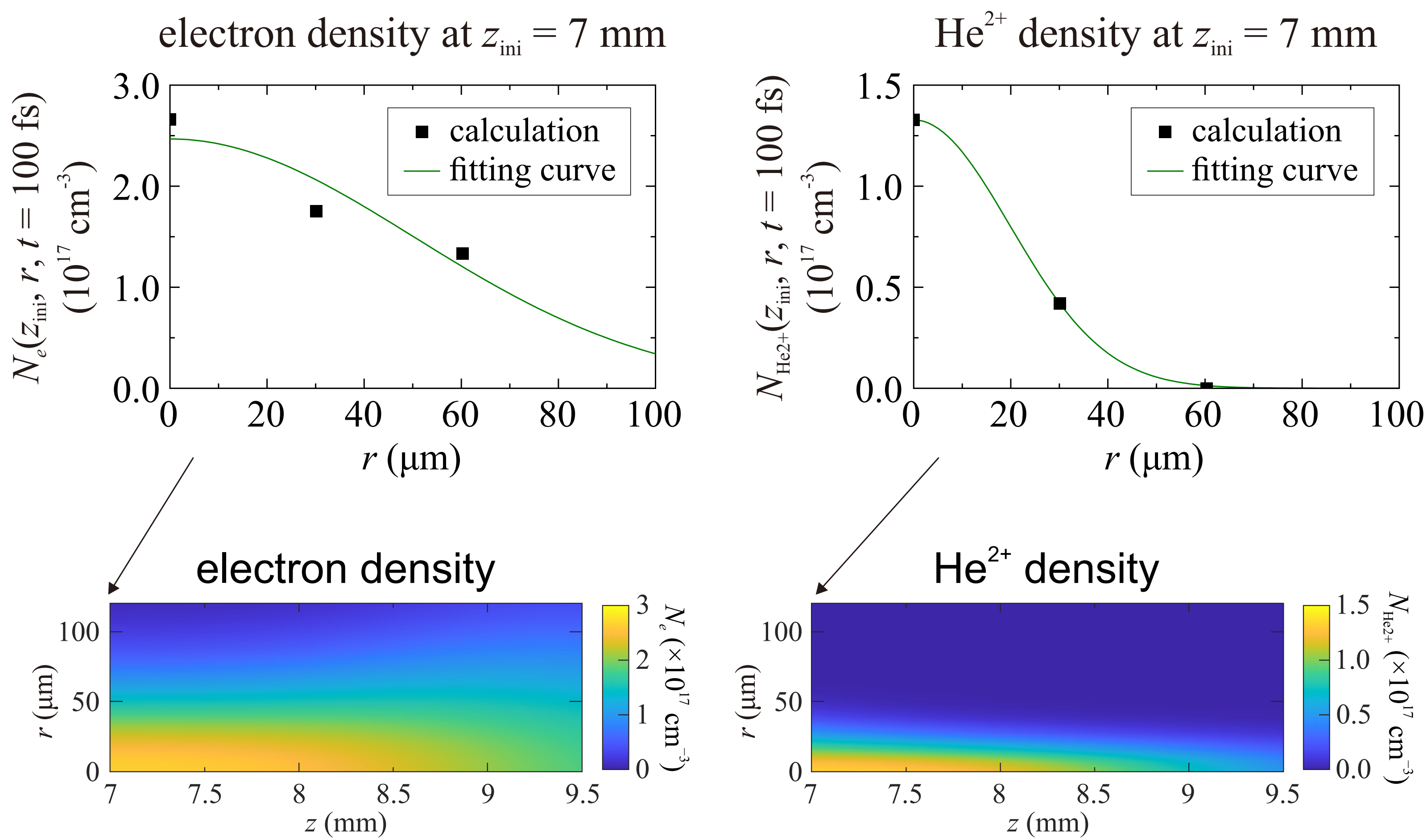

Case 1: 655th (1 keV) harmonic generation

driving pulse energy

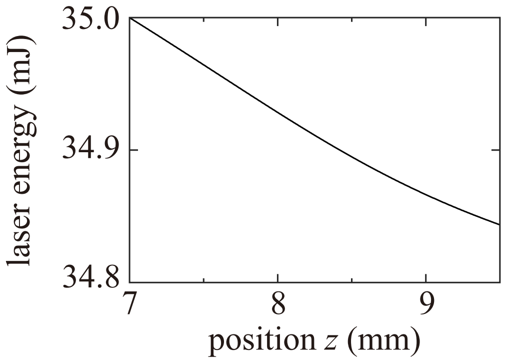

driving beam radius

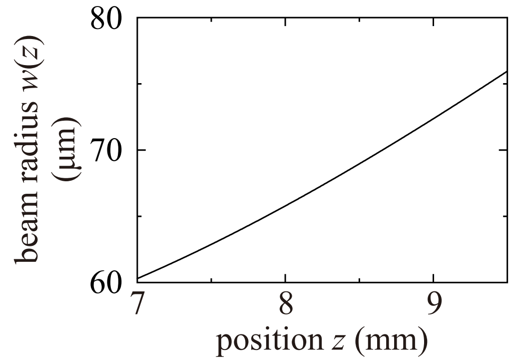

peak intensity

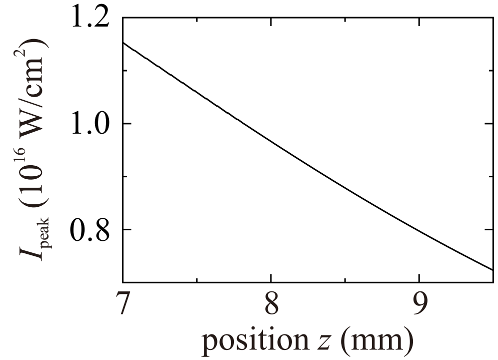

energy loss

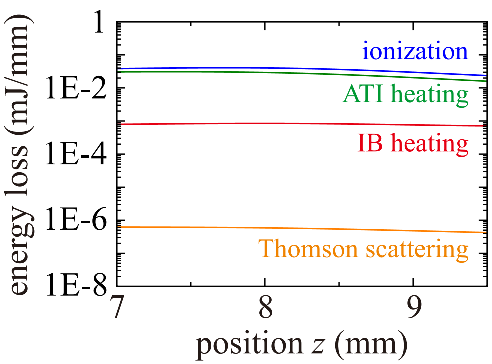

driving pulse duration

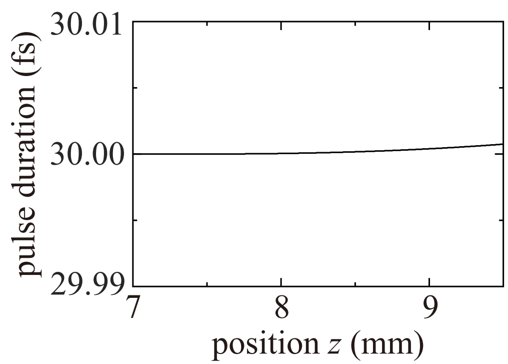

Calculation of harmonic generation

- Trace a fixed harmonic wavefront which is initially generated at $z = z_{ini}$, $r = 0$, and $t = 0$.

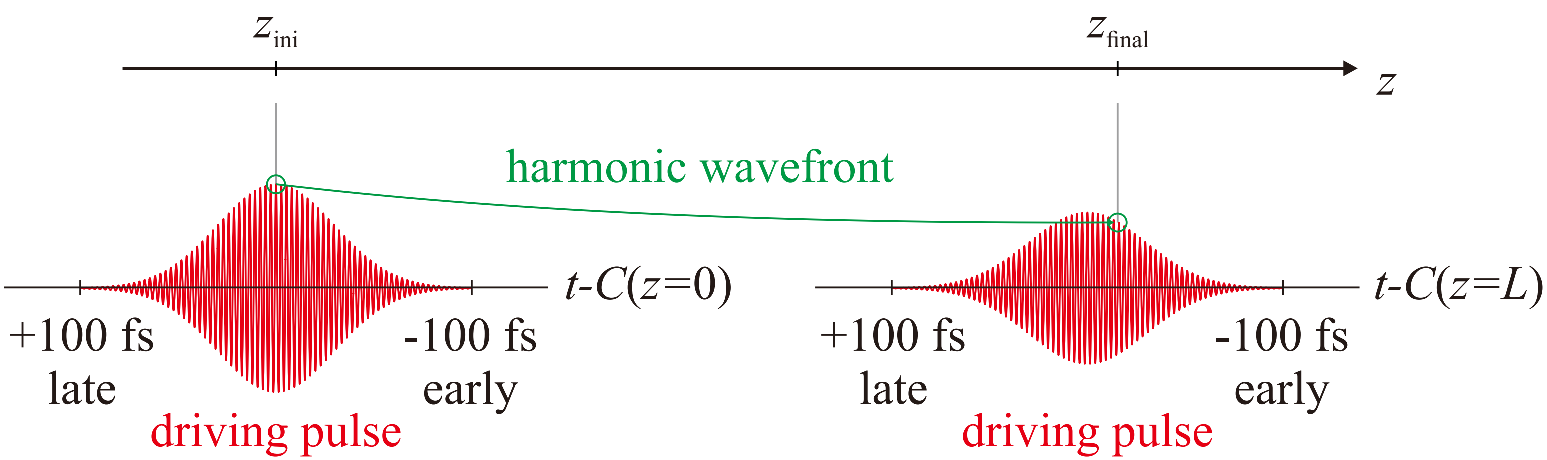

- Driving laser field met by the harmonic wavefront:

$$E_{\text{HWF}}(z) \equiv E_d(z, t_{\text{HWF}}(z))$$

$$t_{\text{HWF}}(z) = \int_0^z \frac{1}{v_p(\omega_q, z')}\, dz' \qquad v_p(\omega_q, z) = \frac{\omega_q}{k(\omega_q, z)}$$

Calculation of harmonic generation

Local harmonic field generated at position z:

$$E_{\mathrm{LH}}(z) \propto N_{\mathrm{source}}(z)\,|E_{\mathrm{HWF}}(z)|^{p}\, e^{i\Phi_{\mathrm{LH}}(z)}$$

empirical constant $p = 5$

Phase of the Local harmonic field:

$$\Phi_{\mathrm{LH}}(z) \equiv q\Phi_{\mathrm{HWF}}(z) + \Phi_{\mathrm{dipole}}(I_d(z))$$

Source density:

$$N_{\mathrm{source}}(z) \propto N_{\mathrm{He}^{1+}}(z, t_{\mathrm{HWF}}(z))\, w_{\mathrm{He}^{1+}}(|E_{\mathrm{HWF}}(z)|)$$

Accumulated harmonic field:

$$E_{\mathrm{HHG}}(z) = \int_0^z E_{\mathrm{LH}}(z')\, dz'$$

Calculation of harmonic generation

- Calculation of the dipole phase:

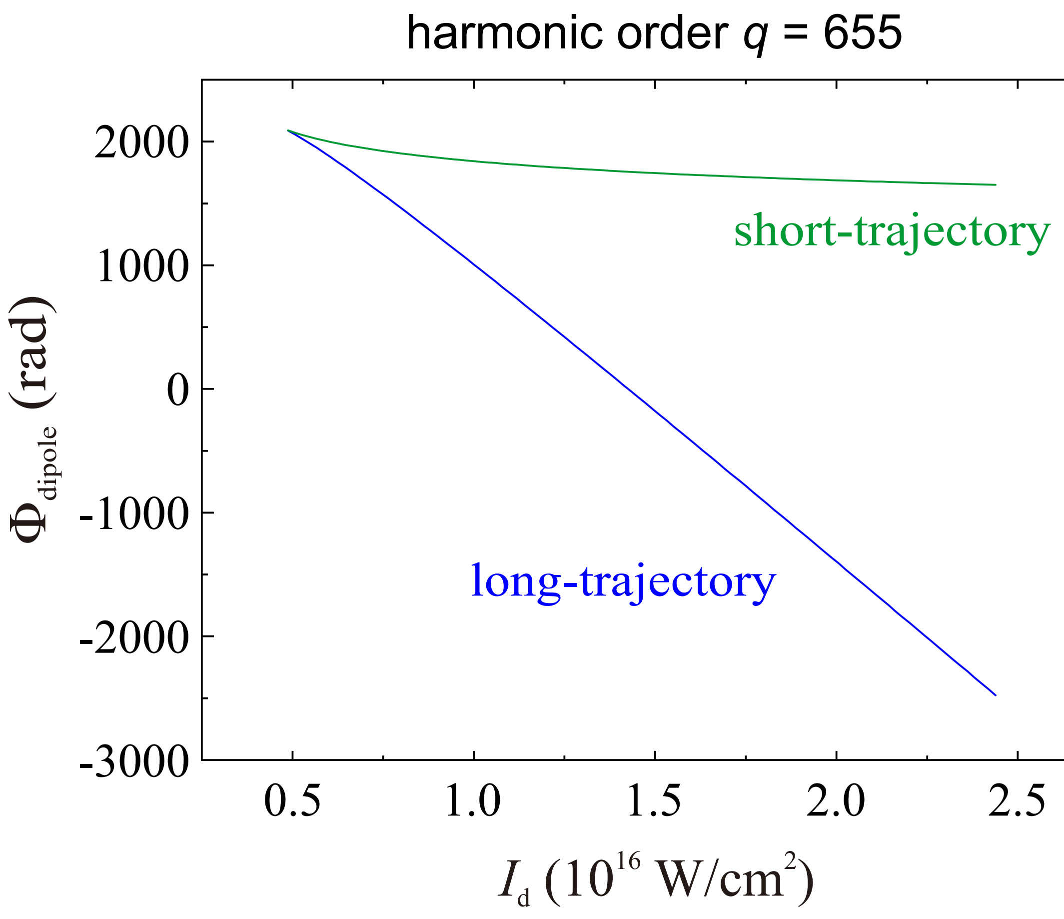

Calculation of harmonic generation

- Calculation of the phase mismatches:

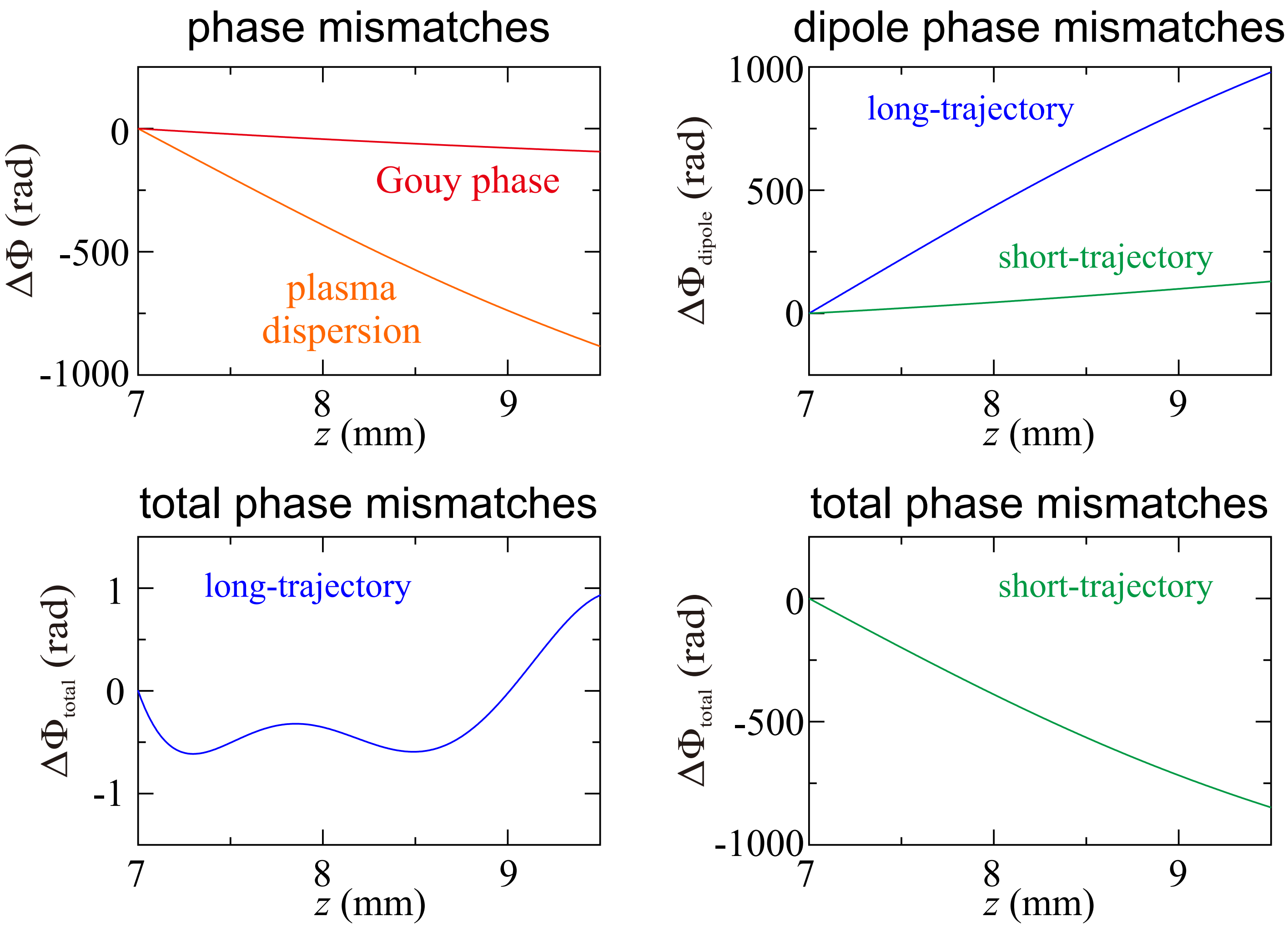

Calculation of harmonic generation

- Calculation of the accumulated harmonic yield

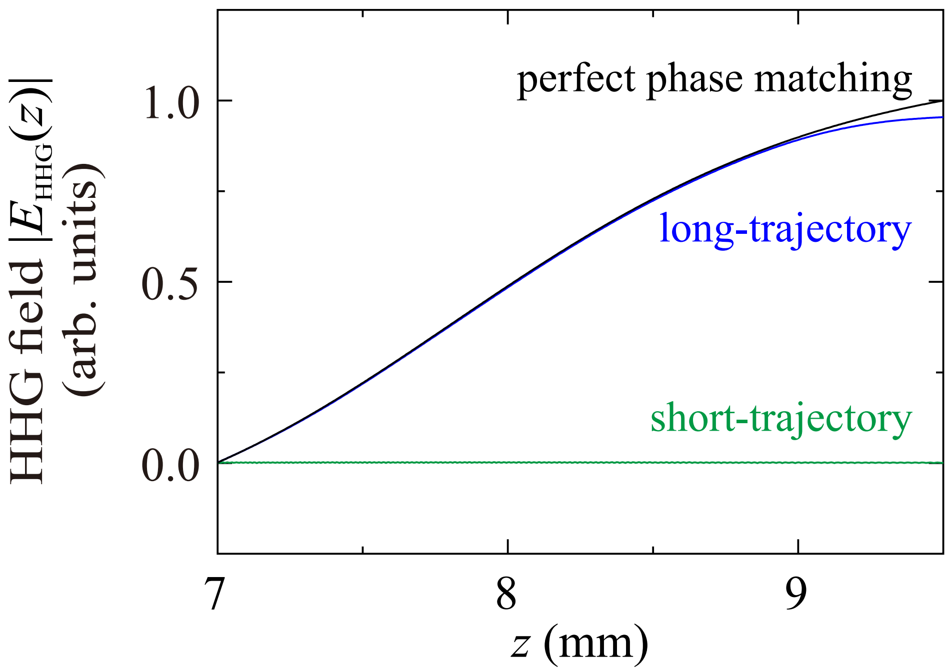

- The amplitude of the long-trajectory harmonic field reaches 95% relative to the ideal condition of perfect phase-matching, corresponding to a relative conversion efficiency of 90%.

Temporal gating effect and bandwidth

- harmonic yield for different harmonic wavefront:

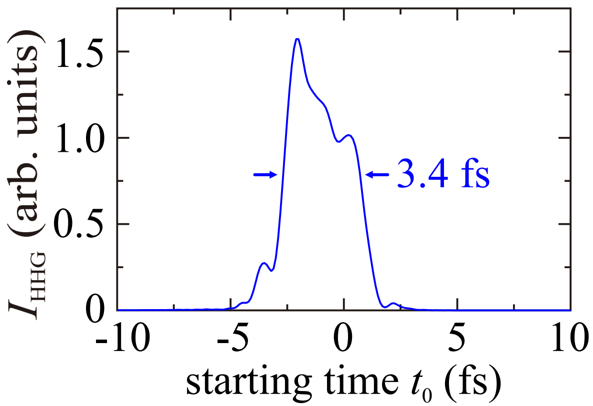

- harmonic yield for different harmonic order:

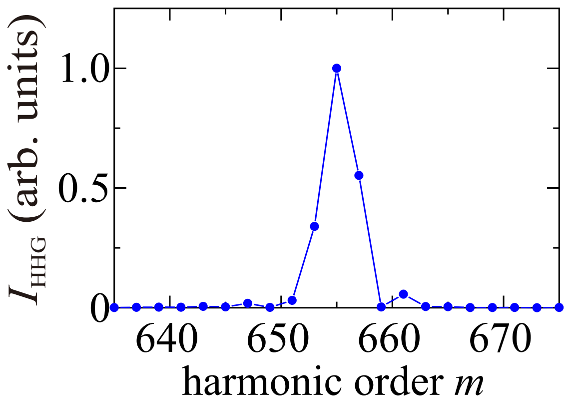

- Since the dipole phase is intensity dependent, the total phase-matching condition varies for different harmonic wavefront initiated at different starting time t_0. Such temporal gating leads to a temporal window of about 3.4-fs width (FWHM).
- The phase-matching bandwidth covers about 3 harmonic orders.

Temporal gating effect and bandwidth

gas jet position z = 18~20.5 mm
pulse duration = 8 fs
wavelength = 810 nm

focal spot waist radius = 55 μm
pulse energy = 22 mJ
He gas density = 7.9×10^{16} cm^{-3}

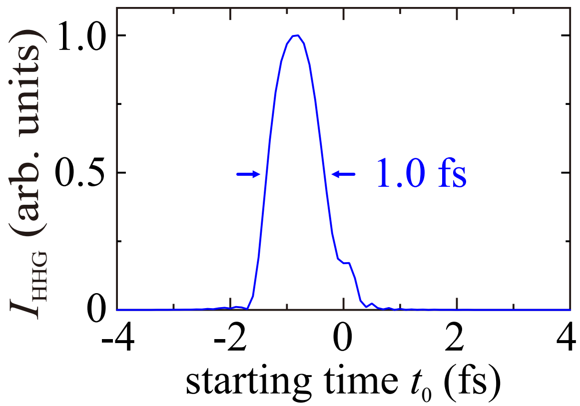

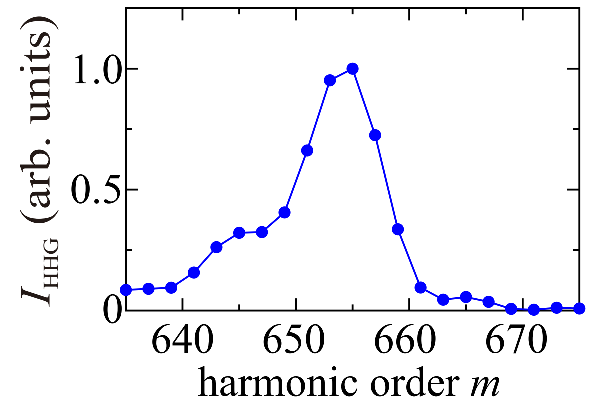

- With a shorter driving pulse duration, the temporal window is shortened to 1.0 fs. The width is shorter than half of the 2.7-fs driving laser period, ensuring that the output HHG will be gated to an isolated attosecond pulse.
- The bandwidth covers about 5 harmonic orders, supporting a pulse duration of about 130 as (FWHM).

Conclusion

- A new scheme of ion-based HHG for 1-keV hard x-ray is proposed.
- The phase-matching condition is achieved by balancing the negative plasma dispersion, Gouy phase shift, and the positive dipole phase variation.
- The intensity-dependent phase-matching condition serves as a temporal gating. Isolated-attosecond-pulse output can be obtained with 8-fs driving pulse duration.
- It would be a promising x-ray source for the research of ultrafast phenomena.